**Research Paper**

# Delayed growth of SK-ES-1 Ewing sarcoma tumors associated with reduced expression and activity of Trk receptors, PI3K, and IGF1R

**Bruna Almeida dos Santos[1, 2, 3], Natália Hogetop Freire[1, 3, 4], Livia Fratini[1], Matheus Dalmolin[3, 5, 6], Josimar Macedo de Castro[7], Marcelo A. C. Fernandes[3, 5, 6, 8], Lauro Gregianin[1, 3, 9, 10], André T. Brunetto[1, 3, 4], Algemir Lunardi Brunetto[1, 3, 4], Luis Fernando da Rosa Rivero[11], Mariane da Cunha Jaeger[1, 3, 4], Rafael Roesler[1, 2, 3, 12, 13], Caroline Brunetto de Farias[1, 2, 3, 4]**

[1] Cancer and Neurobiology Laboratory, Experimental Research Center, Clinical Hospital (CPE-HCPA), Federal University of Rio Grande do Sul, Porto Alegre, RS 90035-003, Brazil
[2] Graduate Program in Biological Sciences: Pharmacology and Therapeutics, Institute for Basic Health Sciences, Federal University of Rio Grande do Sul, Porto Alegre, RS, 90035-003, Brazil
[3] National Science and Technology Institute for Children's Cancer Biology and Pediatric Oncology-INCT BioOncoPed, Porto Alegre, RS, 90035-003, Brazil
[4] Children's Cancer Institute (ICI), Porto Alegre, RS, 90620-110, Brazil
[5] InovAI Lab, nPITI/IMD, Federal University of Rio Grande do Norte, Natal, RN, 59078-970, Brazil
[6] Bioinformatics Multidisciplinary Environment (BioME), Federal University of Rio Grande do Norte, Natal, RN, 59078-970, Brazil
[7] Graduate Program in Medical Sciences, Faculty of Medicine, Federal University of Rio Grande do Sul, Porto Alegre, RS, 90035-003, Brazil
[8] Department of Computer Engineering and Automation, Federal University of Rio Grande do Norte, Natal, RN, 59078-970, Brazil
[9] Department of Pediatrics, Faculty of Medicine, Federal University of Rio Grande do Sul, Porto Alegre, RS, 90035-003, Brazil
[10] Pediatric Oncology Service, Clinical Hospital, Federal University of Rio Grande do Sul, Porto Alegre, RS, 90035-003, Brazil
[11] Department of Pathology, Faculty of Medicine, Federal University of Rio Grande do Sul, Porto Alegre, RS, 90035-003, Brazil
[12] Department of Pharmacology, Institute for Basic Health Sciences, Federal University of Rio Grande do Sul, Porto Alegre, RS, 90035-003, Brazil
[13] Center for Biotechnology, Federal University of Rio Grande do Sul, Porto Alegre, RS, 91501-970, Brazil

***Correspondence to:*** *Caroline Brunetto de Farias,* ***email:*** *cbfarias@zielbiosciences.com*

***Keywords:*** *Ewing sarcoma; K252a; Trk; NTRK; insulin-like growth factor 1 receptor*

**ABSTRACT**

**Ewing sarcoma (ES) is an aggressive childhood tumor. We have previously shown that tropomyosin receptor kinase (Trk) neurotrophin receptors regulate viability, and the pan-Trk and kinase inhibitor K252a restores sensitivity to chemotherapy, in ES cells. Here, we show that administration of K252a in mice delays ES tumor growth and reduces expression and activity of multiple targets. BALB/c nu/nu nude mice inoculated with SK-ES-1 ES cells were given daily intraperitoneal (i.p.) injections of K252a for 18 days. Immunohistochemical analysis of tumors was performed to quantify the expression and phosphorylation of Trk receptors, phosphoinositide 3-kinase (PI3K), and insulin-like growth factor 1 receptor (IGF1R). Associations between genes encoding Trks, PI3G, and IGF1R and overall survival (OS) in patients with ES was examined. Treatment with K252a led to a transient delay in ES tumor growth and reduced the expression and phosphorylation of TrkA, TrkB, PI3K, and IGF1R. Combined treatment with K252a and the IGF1R inhibitor NVP-ADW742 was more effective in reducing ES cell viability than each compound alone. Significant associations between expression of *NTRK* genes and patient OS were found, indicating that *NTRK* genes should be further evaluated as biomarkers for prognosis in patients with ES.**

## INTRODUCTION

Ewing sarcoma (ES) is an aggressive type of childhood cancer that can arise either in bone or soft tissues, with a peak incidence during adolescence, though it also affects younger children and can occur at any age. ES tumors exhibit undifferentiated features that reflect elements of both mesenchymal and neural lineages. Although their exact cellular origin remains debated, current evidence suggests that ES may arise from neural crest–derived or mesenchymal stem cells, and that disruptions in epigenetic programming and multiple signaling pathways during embryonic development can contribute to tumor initiation and progression. At the genetic level, Ewing sarcoma is the prototypical example of a cancer driven by a specific chromosomal translocation. The translocations involve members of the FET (FUS, EWSR1, TAF15) and ETS transcription factor families, most commonly generating the EWS::FLI1 fusion oncogene. The resulting aberrant transcription factor reprograms gene expression and profoundly alters cell fate and differentiation potential, conferring the tumor's hallmark biological behavior. Therapeutically, the introduction of multimodal cytotoxic regimens has markedly improved outcomes for patients with localized disease, yielding survival rates of approximately 70–80%. However, prognosis remains poor for those with metastatic or relapsed ES, with long-term survival dropping to around 30%. Moreover, survivors frequently endure substantial, long-lasting adverse effects from treatment, including growth impairment, organ toxicity, and limb amputations, alongside the emotional and social challenges that come with surviving a severe childhood cancer [1-6].

Given that the oncogenic fusion protein EWS::FLI1 by itself is hard to directly target with drugs, other components of the ES cell signaling landscape have been investigated as therapeutic targets. These include cell surface receptors such as receptor tyrosine kinases (RTKs) [7-10]. Members of the RTK subfamily, tropomyosin receptor kinase (Trk) receptors include TrkA, TrkB, and TrkC, which are encoded by the *NTRK1*, *NTRK2*, and *NTRK3* genes, respectively. TrkA is the high-affinity receptor for nerve growth factor (NGF), while TrkB primarily binds brain-derived neurotrophic factor (BDNF) and neurotrophin-4 (NT-4). Neurotrophin-3 (NT-3) has the highest affinity for TrkC but can also to a lesser degree activate TrkA and TrkB. Upon ligand binding, Trk receptors undergo homodimerization and autophosphorylation at specific tyrosine residues, stimulating downstream cell signaling cascades that include the phosphoinositide 3-kinase (PI3K), mitogen-activated protein kinase (MAPK), and phospholipase C-γ (PLCγ)/protein kinase C (PKC) pathways [11-12]. Beyond their physiological roles in the nervous system, Trk receptors have been increasingly implicated in tumor progression, therapy resistance, and cell survival in several types of cancer [13-17]. Trk inhibitors larotrectinib and entrectinib are currently used to treat patients with tumors harboring *NTRK* gene fusions, regardless of cancer type [13, 18-21].

In sarcomas, *NTRK* fusion genes were first identified in infantile fibrosarcoma (IFS), which can harbor a canonical *ETV6-NTRK3* gene fusion [22, 23]. Current evidence demonstrates various *NTRK1* and *NTRK3* fusion genes in IFS and other sarcoma types [23, 24]. TRK fusion proteins show activation of the kinase domain, which can lead to constitutive activation of PI3K and MAPK signaling through a mechanism dependent on insulin-like growth factor 1 receptors (IGF1R) [23, 25]. Patients with *NTRK* fusion-positive IFS tumors show a 96% response rate to larotrectinib, indicating that *NTRK* fusions define a molecular subset of sarcoma tumors highly sensitive to Trk inhibitors [26].

In a previous study, we reported that TrkA and TrkB are expressed in ES tumors, and treating ES cells to selective TrkA or TrkB inhibitors reduced cell proliferation, an effect that was increased when TrkA and TrkB were blocked simultaneously [27]. We then used the furanosylated indolocarbazole K252a, a microbial alkaloid originally isolated from the soil fungi *Nocardiopisis sp.* and structurally related to staurosporine, as a pan-Trk inhibitor [28-31]. Treatment with K252a induced changes in cell morphology, reduced β-III tubulin levels, and decreased mRNA expression of NGF, BDNF, TrkA and TrkB. In addition, combining K252a with subeffective doses of cytotoxic chemotherapeutic drugs resulted in decreased ES cell proliferation and survival and restored sensitivity to chemotherapy in chemoresistant ES cells [27]. Here, we show that treatment with K252a delays ES tumor growth in mice and the effect is associated with inhibition of multiple tumor targets.

## RESULTS

### Systemic administration of K252a produces a transient delay in ES tumor growth

Treating nude mice inoculated with human SK-ES-1 ES cells with daily injections of K252a resulted in a significant reduction in tumor growth during treatment compared to controls. There were significant effects of treatment and time as well significant interactions between these factors (all *p*s < 0.01; Figure 1B, 1C). The halt in tumor growth was apparent between treatment days 9 and 15. However, by day 18, tumor size in the treatment group had recovered to levels comparable to those observed in the control group, suggesting that the drug effect was transient (Figure 1B). There were no significant differences between groups in body weight (Figure 1D) or serum biochemical markers, although apparent reductions in AST and ALT levels were observed in K252a-treated mice (Figure 1E-H).

**Figure 1 should be inserted here**

### Treatment with K252a reduces the protein expression and phosphorylation of TrkA, TrkB, PI3K, and IGF1R, without affecting TrkC in ES tumors

Tumors from mice treated with K252a had reduced protein levels of total (Figure 2) and phosphorylated (Figure 3) TrkA (total, $p = 0.06$, phosphorylated, $p = 0.04$), TrkB (total, $p = 0.05$, phosphorylated, $p = 0.012$), and PI3K (total, $p = 0.05$, phosphorylated, $p = 0.02$), but unchanged TrkC levels. A subsequent analysis showed that K252a also reduced total and phosphorylated levels of IGF1R (total, $p = 0.02$, phosphorylated, $p = 0.01$; Figure 4A, 4B). Significant correlations were found in reduction of protein

expression between several pairs of targets in cohorts of ES tumors from both groups of mice (Supplementary Figure S1).

**Figure 2 should be inserted here**

**Figure 3 should be inserted here**

## Combination treatment with K252a and an IGF1R inhibitor reduces ES cell viability

Exposure to K252a or NVP-ADW742 at doses equivalent to the IC10 resulted in a small but statistically significant reduction in the viability of SK-ES-1 ES cells. When the two drugs were used in combination, the resulting inhibition of cell viability was significantly more pronounced compared to the effects of each drug given alone (all *p*s < 0.05, Figure 4C). Significant synergism was demonstrated between the two drugs (25 and 75% quantiles = 19.29, Figure 4D).

**Figure 4 should be inserted here**

## NTRK gene expression is associated with OS in patients with ES

TrkB, encoded by the *NTRK2* gene, is considered a preferred target of K252a inhibition. We found that higher *NTRK2* transcription is associated with worse prognosis assessed by shorter OS, specifically in the COG cohort ($p$ = 0.0042, Figure 5C). In contrast, high *NTRK1* expression was associated with longer OS in the EuroEwing cohort ($p$ = 0.0049, Figure 5B). *NTRK3* showed opposite patterns of association in the two datasets, indicating shorter OS in the COG cohort ($p$ = 0.0052, Figure 5E) but longer OS in the EuroEwing cohort ($p$ = 0.013, Figure 5F). No significant associations between gene expression and OS were found for *PIK3CA* (Supplementary Figure S2A, S2B), *PIK3R1* (Supplementary Figure S2C, S2D), or *IGF1R* (Supplementary Figure S3).

**Figure 5 should be inserted here**

## DISCUSSION

K252a has been widely used as a tool to investigate Trk-mediated signaling, particularly for TrkB, due to its potent inhibitory effects on Trks at nanomolar concentrations. However, at higher or even similar concentrations, and certainly at the doses we used in our *in vivo* experiment, it can also directly inhibit several other protein kinases [32-36]. Therefore, it is more accurate to interpret our findings as reflecting the effects of a non-specific, multi-kinase inhibitor, rather than those of a TrkB or pan-Trk inhibitor. Administration of K252a was able to significantly reduce the protein content and phosphorylation (a biochemical surrogate for kinase activation) of TrkA, TrkB, PI3K, and IGF1R in SK-ES-1 ES tumor xenografts, raising the possibility that either direct or indirect inhibition of these targets at least partially mediates the effect of K252a on tumor growth. Our correlation analysis showed that the expression of p-PI3K was positively associated with the content of both p-TrkA and p-TrkB, supporting the possibility that PI3K is among the downstream targets of Trk inhibition. Some of the main findings from the animal and cellular experiments reported in this study are summarized in Figure 6.

One critical aspect of our findings was the transient nature of the antitumor effect of K252a. Tumors can rapidly acquire resistance to other Trk inhibitors through recurrent mutations in the Trk kinase domain [37]. However, it is more likely that rapid acquisition of resistance occurred through biochemical compensatory changes, rather than genetic alterations which can take longer to manifest. It has been shown that neuroblastoma cells overexpressing TrkB can developed resistance to entrectinib, a pan-TRK, anaplastic lymphoma kinase (ALK), and proto-oncogene tyrosine-protein kinase ROS (ROS1) inhibitor, by adaptations including activation of MAPK, downregulation of PTEN, and IGF1R activation. These changes allow preservation of downstream TrkB signaling in the presence of entrectinib [38]. It is also possible that the treatment rapidly selected for pre-existing resistant cells within the tumor.

Consistent with the possibility, raised by our previous study [27], that TrkA and TrkB expression and signaling influence ES growth, we found that higher *NTRK2* gene expression can be associated with worse prognosis assessed by OS, whereas high *NTRK1* expression indicates longer OS. These effects were observed specifically in one of the two cohorts examined, so that significant effects were found for *NTRK1* in the EuroEwing dataset and for *NTRK2* in the COG dataset. Contrasting patterns between the two patient cohorts were found for *NTRK3*; high gene expression was associated with a shorter OS in the COG dataset but longer OS in the EuroEwing dataset. We previously found a similar association between high *NTRK3* transcription and longer survival in patients with medulloblastoma, the main type of pediatric brain tumor [17]. Both *NTRK1* and *NTRK3* can act either as oncogenes or tumor suppressor genes. *NTRK1* is a tumor suppressor inhibited by methylation in ovarian cancer and endometrial hyperplasia [39, 40]. Reconstitution of normal *NTRK3* expression previously suppressed by aberrant hypermethylation induces apoptosis in colon tumors [41], and *NTRK3* is a tumor suppressor gene inactivated by methylation also in cervical cancer [42]. However, the first study reporting a role for the *NTRK3* product, TrkC, in ES found the receptor to be frequently overexpressed in human metastatic ES cells, promoting cell survival, tumorigenicity, and metastasis, and loss of TrkC expression reduced experimental ES tumor growth and metastasis in mice [43]. Although *NTRK* gene fusions are mutually exclusive with the translocations that define ES [44], our previous *in vitro* findings and current results support the possibility that Trk inhibition can reduce ES growth even in the absence of pathological gene fusions.

Overexpression of IGF1R has been associated with more aggressive tumors and worse outcomes in ES, although our own transcriptional analysis did not reveal an association between IGF1R mRNA expression and survival of ES patients. Monoclonal antibodies targeting IGF1R have been developed and tested clinically in patients with ES in several trials, although the clinical efficacy remains to be fully established [45-50]. IGF1R activation enhances the expression of TrkA and TrkB at the mRNA and protein levels [51], and IGF1R functionally interacts with Trks in regulating drug resistance [25, 38]. Another novel finding reported in the present study is that the combination of K252a with an IGF1R inhibitor was more efficient in reducing ES cell viability than each drug given alone, highlighting the importance of evaluating combinatorial therapeutic regimens involving IGF1R inhibitors and drugs targeting Trks and protein kinases [52]. SK-ES-1 cells are derived from an ES tumor occurring in the bone of a 18 year-old male patient [53]. We describe the successful growth of ES tumors using SK-ES-1 cells xenografted into nude mice. Previous studies have used and validated SK-ES-1 xenografts as a preclinical model of ES [54, 55]. However, one of the limitations of our study is that patient-derived xenograft (PDX) mouse models, defined as models developed from direct implantation of patient tumor tissue into immunodeficient mice without prior cell culture or expansion, are now considered the gold standard for *in vivo* preclinical drug testing, and a number of such models have been developed for ES and other pediatric solid tumors [56]. It is also worth noting that our experiments do not allow to determine whether the reductions in target expression and phosphorylation are due to direct inhibition by K252a or downstream to drug-induced inhibition of Trks or other kinases. Future experiments should explore in detail the effects of selective TrkA, TrkB, and PI3K inhibitors, and compare them with multi-kinase inhibitors.

In summary, we report evidence suggesting that the combined inhibition of Trks, PI3K, and IGF1R by a multi-kinase inhibitor can delay ES tumor growth. In addition, NTRK genes should be further evaluated as potential biomarkers for prognosis in patients with ES.

**Figure 6 should be inserted here**

## MATERIALS AND METHODS

### Ethics statement

All experimental procedures with animals were conducted in accordance with the guidelines established by the National Council for Animal Control and Experimentation (CONCEA, Ministry of Science, Technology and Innovation, Brazil), as well as with Animal Research: Reporting of In Vivo Experiments (ARRIVE) guidelines. All protocols used in this study were approved by the institutional Animal Care and Use Committee (CEUA, Hospital de Clínicas de Porto Alegre-HCPA), under project number 2019/0638, approved February 19, 2020).

### Cell culture

SK-ES-1 ES cells obtained from the American Type Cell Collection (ATCC® HTB-86™) were verified for authenticity by Short Tandem Repeat (STR) and lack of contamination. Cells were cultured and incubated in 5% $CO_2$ at 37°C in RPMI-1640

Medium (Gibco™, Thermo Fisher Scientific, Waltham, USA), supplemented with 1% amphotericin B, 5% 10,000 Ul/mL penicillin 10 mg/ml streptomycin, and 10% fetal bovine serum (FBS, Gibco™, Thermo Fisher Scientific).

**Drug treatment**

K252a, methyl (13S,14R,16R)-14-hydroxy-13-methyl-5-oxo-6,7,13,14,15,16-hexahydro-5H-13,16-epoxydiindolo[1,2,3-fg:3′,2′,1′-kl]pyrrolo[3,4-i][1,6]benzodiazocine-14-carboxylate, (Sigma Aldrich, St. Louis, USA) and the selective IGF1R inhibitor NVP-ADW742 (Sigma Aldrich) were dissolved in dimethyl sulfoxide (DMSO, Sigma Aldrich). K252a was dissolved in saline solution (NaCl 0.9%) at the concentration of 2% DMSO in 98% saline for the treatment of mice at a dose of 0.5 mg/kg. Control mice were given vehicle (2% DMSO in 98% saline). For *in vitro* assays, cells were treated with the inhibitory concentration of 10% (IC10) of K252a (10 nM), NVP-ADW742 (196.6 nM) or K252a plus NVP-ADW742. Control cells were exposed to vehicle (DMSO 0.2%) in the culture medium.

**Xenograft assay**

Six-week-old male nude mice (BALB/c nu/nu) from our own institutional breeding colony were used for the *in vivo* experiments. Mice were randomly distributed into two groups, K252a treatment and control. A cell line-derived tumor xenograft (CDX) model was used to induce tumors. Animals were inoculated subcutaneously (s.c..) on the right dorsal flank with a suspension of SK-ES-1 cells ($3 \times 10^6$). After the tumors reached 80 $mm^3$-100$mm^3$, the mice received intraperitoneal (i.p.) injections with K252a (0.5 mg/kg/day) or the same volume of vehicle (2% DMSO in 98% saline) once daily during 18 days. Body weight (g), tumor width (W) and tumor length (L) were measured every three days until treatment day 18, and tumor volume (mm3) was determined by the formula $(W^2 \times L)/2$. At the end of the treatment, the mice were euthanized under deep isoflurane anesthesia and the blood and tumors were collected for biochemical and histological analysis.

**Biochemical markers**

Heart blood was collected via puncture pre-euthanasia and serum was separated (at 3,000 rpm for 10 min) and stored at −80 °C. Alanine aminotransferase (ALT), aspartate aminotransferase (AST), creatinine and urea serum levels were evaluated by closed-circuit photometric assays (Cobas® c702, F. Hoffmann-La Roche Ltd., Basel, Switzerland).

**Immunohistochemistry on tissue microarrays (TMA)**

Tumors ($n$ = 7 per group, removed immediately after the mouse's death) were fixed in 10% formalin to be included in paraffin blocks. Sections of three micrometers were used for the production of slides stained with hematoxylin-eosin (HE) as they served to evaluate the morphology and an area for the fabrication of the tissue microarray (TMA). A 2 mm block of TMA was used for the study, where duplicates were posted as the source area. Ten antibodies were used: TrkA polyclonal antibody (Product # PA5-90581), TrkB polyclonal antibody (Product # PA5-88293), phospho-TrkA (Tyr791) polyclonal antibody (Product # PA5-105456), TrkC polyclonal antibody pTyr516

(Product # PA5-39755), phospho-IGF1R polyclonal antibody (Tyr1165, Tyr1166) (Product # PA5-104772), PI3K p85 alpha polyclonal antibody (Product # PA5-29220), phospho-PI3 kinase p85 alpha pTyr607 polyclonal antibody (Product # PA5-38905), phospho-TrkB polyclonal antibody pTyr515 (Product # PA5-38076), TrkC polyclonal antibody (Product # PA5-79766), TrkC polyclonal antibody (Product # PA5-79766), IGF1R (CD221) polyclonal antibody (Product # PA5-79445), and an anti-rabbit secondary antibody. The immunohistochemistry (IHC) protocol was carried out according to the specifications of each data sheet. The IHC assessment was scored semi-quantitatively according to intensity and distribution.

**Cell viability**

SK-ES-1 ES cells were seeded at a density of 4 X 103 cells per well in a complete medium into 96-well plates (Kasvi, Pinhais, Brazil). After 24 h, cells were treated with K252a, NVP-ADW742, or the two drugs combined, for 72 h and the medium was then removed, cells were washed with phosphate-buffered saline (PBS) and detached with 0.25% trypsin solution (Gibco™, Thermo Fisher Scientific). For cell viability analysis, the cell suspension was homogenized with trypan blue (BioSumos, Porto Alegre, Brazil) and counted in a hemocytometer. The mean of three independent experiments for each dose was used to calculate dose-response and combination index values.

**Drug interactions**

The combination index between the effects of K252a and NVP-ADW742 was calculated using the SinergyFinder/R version 4.1.3 package [57], with cell viability of SK-ES-1 ES cells as input using the ZIP (Zero Interaction Potency) method.

**Gene expression and survival analysis in ES patients**

The gene expression dataset used for the survival analysis were obtained from the Gene Expression Omnibus (GEO) datasets accession numbers GSE63155 and GSE63156. The datasets GSE63155 and GSE63156 comprise expression data (Affymetrix Human Exon 1.0 ST Array) from primary ES tumor biopsies obtained from 46 patients from the Children's Oncology Group (COG) and 39 patients from the EuroEwing collaborative group respectively [58]. Microarray raw data (GSE63155 and GSE63156, Affymetrix Human Exon 1.0 ST Array, GPL5175) normalization (Robust Multichip Average, RMA method) and quality control were performed using the oligo Bioconductor/R version 4.3.1). Overall survival (OS) analysis for ES patients was done by Kaplan-Meier curves using the ‘Survival’ and ‘Survminer’ packages, to evaluate the effects of expression of each gene of interest namely the *NTRK1*, *NTRK2*, *NTRK3*, *IGF1R*, *PIK3CA* (which encodes the p110α protein, the catalytic subunit of the PI3K), and *PIK3R1* (which encodes a regulatory subunit of PI3K).

**Statistical analysis**

The Shapiro-Wilk test and histograms were used to verify the distribution of variables. An independent t-test was used for comparisons between groups, assuming a parametric distribution. Repeated measurements (body weight and tumor volume) were assessed by the Generalized Estimating Equation (GEE). The GEE model was modeled to identify statistical differences between treatment groups in mice (K252a versus

controls), as well as tumor volume between treatment days and the interaction between both factors. In the presence of a significant interaction indicated by $p < 0.05$, Bonferroni's correction was used for post-hoc multiple comparisons. The ordinal histology variables were analyzed using the Spearman's correlation method. All analyses were performed using the SPSS 20.0 software (IBM, Armonk, USA), assuming significance level at $p < 0.05$. Data are presented as mean and + standard error of the mean (S.E.M.).

## DATA AVAILABILITY

The ES tumor datasets GSE63155 and GSE63156, 28 used for the analyses of associations between gene expression and patient survival presented in this study, are available at https://www.ncbi.nlm.nih.gov/geo/query/acc.cgi?acc=GSE63155 and https://www.ncbi.nlm.nih.gov/geo/query/acc.cgi?acc=GSE63156, respectively. Other data presented in this study may be obtained from the corresponding author upon request.

## SUPPLEMENTARY MATERIALS

The following supporting information is provided: Supplementary Figure S1; Supplementary Figure S2; Supplementary Figure S3.

## AUTHOR CONTRIBUTIONS

Conceptualization, B.A.S. and C.B.F.; methodology, B.A.S., N.H.F., L.F., M.D., J.M.C., L.F.R.R., and M.C.J.; validation, M.A.C.F., M.C.J., and C.B.F.; formal analysis, B.A.S., C.B.F., M.D., and J.M.C.; investigation, B.A.S., N.H.F., L.F., M.D., J.M.C., L.F.R.R., and M.C.J.; resources, M.A.C.F., A.T.B., A.L.B., M.C.J., R.R., and C.B.F.; data curation, B.A.S., C.B.F., M.D., and J.M.C.; writing—original draft preparation, B.A.S., C.B.F. M.D., and R.R.; writing—review and editing, B.A.S., N.H.F., L.F., M.D., J.M.C., M.A.C.F., L.G., A.T.B., A.L.B., L.F.R.R. M.C.J., R.R., C.B.F.; supervision, M.A.C.F., L.G., A.T.B., A.L.B., R.R., C.B.F.; project administration, C.B.F.; funding acquisition, A.T.B., A.L.B., M.C.J., R.R., C.B.F. All authors have read and agreed to the published version of the manuscript.

## CONFLICTS OF INTEREST

The authors declare no conflicts of interest.

## FUNDING

This research was supported by PRONON/Ministry of Health, Brazil (number 25000.202751/2016-65); National Council for Scientific and Technological Development (CNPq) grant numbers 304623/2025-3 and 406484/2022-8-INCT BioOncoPed to R.R.; the Children's Cancer Institute (ICI); the Coordination for the Improvement of Higher Education Personnel (CAPES); and the Clinical Hospital institutional research fund (FIPE-HCPA number 20190638).

## INSTITUTIONAL REVIEW BOARD STATEMENT

All experimental procedures involving mice were conducted in accordance with the guidelines established by the National Council for Animal Control and Experimentation (CONCEA, Ministry of Science, Technology and Innovation, Brazil), as well as with Animal Research: Reporting of In Vivo Experiments (ARRIVE) guidelines. All protocols used in this study were approved by the institutional Animal Care and Use Committee (CEUA, Hospital de Clínicas de Porto Alegre-HCPA), under project number 2019/0638, approved February 19, 2020.

## REFERENCES


1. dos Santos RP, Roesler R, Gregianin L, Brunetto AT, Jaeger M, Brunetto AL, de Farias CB. Cancer stem cells and chemoresistance in Ewing sarcoma. Curr Stem Cell Res Ther. 2023; 18:926-36. doi: 10.2174/1574888X17666220627114710
2. Dupuy M, Lamoureux F, Mullard M, Postec A, Regnier L, Baud'huin M, Georges S, Brounais-Le Royer B, Ory B, Rédini F, Verrecchia F. Ewing sarcoma from molecular biology to the clinic. Front Cell Dev Biol. 2023; 11:1248753. doi: 10.3389/fcell.2023.1248753
3. Gregianin LJ, Rose A, Villarroel M, Almeida MT, Siqueira L, Salgado C, da Costa GA, Castillo L, Santos Pestilho JFC, Brunetto AL. GALOP Latin American Pediatric Oncology Group Ewing Sarcoma Investigators. Results of the Latin American Pediatric Oncology Group (GALOP-2011) trial for patients with localized Ewing sarcoma: A multicentric study of interval-compressed multiagent chemotherapy. Pediatr Blood Cancer. 2025; 72:e31554. doi: 10.1002/pbc.31554
4. Gupta A, Dietz MS, Riedel RF, Dhir A, Borinstein SC, Isakoff MS, Aye JM, Rainusso N, Armstrong AE, DuBois SG, Wagner LM, Rosenblum JM, Cohen-Gogo S, Albert CM, Zahler S, Chugh R, Trucco M. Consensus recommendations for systemic therapies in the management of relapsed Ewing sarcoma: A report from the National Ewing Sarcoma Tumor Board. Cancer. 2024; 130:4028-39. doi: 10.1002/cncr.35537
5. Riggi N, Suvà ML, Stamenkovic I. Ewing's Sarcoma. N Engl J Med. 2021; 384:154-64. doi: 10.1056/NEJMra2028910
6. Zöllner SK, Amatruda JF, Bauer S, Collaud S, de Álava E, DuBois SG, Hardes J, Hartmann W, Kovar H, Metzler M, Shulman DS, Streitbürger A, Timmermann B, Toretsky JA, Uhlenbruch Y, Vieth V, Grünewald TGP, Dirksen U. Ewing sarcoma-diagnosis, treatment, clinical challenges and future perspectives. J Clin Med. 2021; 10:1685. doi: 10.3390/jcm10081685
7. Daley JD, Whiteway SL, Heske CM, Dela Cruz FS, Whittle SB, Cohen-Gogo S, Collier AB, Gupta A, Ohm J, Clark A, Soragni A, Lawlor E, Setty B, Grohar PJ, Janeway K, Reed DR, Slotkin EK, Bailey KM. New approaches to investigate novel agents in Ewing sarcoma: A report from the Children's Oncology Group Bone Tumor Committee. Pediatr Blood Cancer. 2025; 72:e31917. doi: 10.1002/pbc.31917
8. Fayzullina D, Tsibulnikov S, Stempen M, Schroeder BA, Kumar N, Kharwar RK, Acharya A, Timashev P, Ulasov I. Novel targeted therapeutic strategies for Ewing sarcoma. Cancers (Basel). 2022; 14:1988. doi: 10.3390/cancers14081988
9. Jia K, Cao L, Yu Y, Jing D, Wu W, Van Tine BA, Shao Z. Signaling pathways and targeted therapies in Ewing sarcoma. Pharmacol Ther. 2025; 266:108765. doi: 10.1016/j.pharmthera.2024.108765
10. Just MA, Van Mater D, Wagner LM. Receptor tyrosine kinase inhibitors for the treatment of osteosarcoma and Ewing sarcoma. Pediatr Blood Cancer. 2021; 68:e29084. doi: 10.1002/pbc.29084
11. Bothwell M. Recent advances in understanding neurotrophin signaling. F1000Res. 2016; 5:F1000 Faculty Rev-1885. doi: 10.12688/f1000research.8434.1
12. Park H, Poo MM. Neurotrophin regulation of neural circuit development and function. Nat Rev Neurosci. 2013; 14:7-23. doi: 10.1038/nrn3379
13. Amatu A, Sartore-Bianchi A, Bencardino K, Pizzutilo EG, Tosi F, Siena S. Tropomyosin receptor kinase (TRK) biology and the role of NTRK gene fusions in cancer. Ann Oncol. 2019; 30(Suppl_8):viii5-5. doi: 10.1093/annonc/mdz383

14. Meldolesi J. Neurotrophin Trk receptors: New targets for cancer therapy. Rev Physiol Biochem Pharmacol. 2018; 174:67-79. doi: 10.1007/112_2017_6
15. Roesler R, de Farias CB, Abujamra AL, Brunetto AL, Schwartsmann G. BDNF/TrkB signaling as an anti-tumor target. Expert Rev Anticancer Ther. 2011; 11:1473-5. doi: 10.1586/era.11.150
16. Thiele CJ, Li Z, McKee AE. On Trk--the TrkB signal transduction pathway is an increasingly important target in cancer biology. Clin Cancer Res. 2009; 15:5962-7. doi: 10.1158/1078-0432.CCR-08-0651
17. Thomaz A, Jaeger M, Brunetto AL, Brunetto AT, Gregianin L, de Farias CB, Ramaswamy V, Nör C, Taylor MD, Roesler R. Neurotrophin signaling in medulloblastoma. Cancers (Basel). 2020; 12:2542. doi: 10.3390/cancers12092542
18. Amatu A, Sartore-Bianchi A, Siena S. NTRK gene fusions as novel targets of cancer therapy across multiple tumour types. ESMO Open. 2016; 1:e000023. doi: 10.1136/esmoopen-2015-000023
19. Drilon A, Laetsch TW, Kummar S, DuBois SG, Lassen UN, Demetri GD, Nathenson M, Doebele RC, Farago AF, Pappo AS, Turpin B, Dowlati A, Brose MS, Mascarenhas L, Federman N, Berlin J, El-Deiry WS, Baik C, Deeken J, Boni V, Nagasubramanian R, Taylor M, Rudzinski ER, Meric-Bernstam F, Sohal DPS, Ma PC, Raez LE, Hechtman JF, Benayed R, Ladanyi M, Tuch BB, Ebata K, Cruickshank S, Ku NC, Cox MC, Hawkins DS, Hong DS, Hyman DM. Efficacy of larotrectinib in TRK fusion-positive cancers in adults and children. N Engl J Med. 2018; 378:731-9. doi: 10.1056/NEJMoa1714448
20. Laetsch TW, Hong DS. Tropomyosin receptor kinase inhibitors for the treatment of TRK fusion cancer. Clin Cancer Res. 2021; 27:4974-82. doi: 10.1158/1078-0432.CCR-21-0465
21. Nasehi P, Omidkhah N, Ghodsi R. A review: Recent developments of co-targeted TRK (tropomyosin receptor kinases) inhibitors for cancer therapy. Bioorg Chem. 2025; 165:108950. doi: 10.1016/j.bioorg.2025.108950
22. Knezevich SR, McFadden DE, Tao W, Lim JF, Sorensen PH. A novel ETV6-NTRK3 gene fusion in congenital fibrosarcoma. Nat Genet. 1998; 18:184-7. doi: 10.1038/ng0298-184
23. Kubota Y, Kawano M, Iwasaki T, Itonaga I, Kaku N, Ozaki T, Tanaka K. Current management of neurotrophic receptor tyrosine kinase fusion-positive sarcoma: an updated review. Jpn J Clin Oncol. 2025; 55:313-26. doi: 10.1093/jjco/hyaf015
24. Doebele RC, Davis LE, Vaishnavi A, Le AT, Estrada-Bernal A, Keysar S, Jimeno A, Varella-Garcia M, Aisner DL, Li Y, Stephens PJ, Morosini D, Tuch BB, Fernandes M, Nanda N, Low JA. An oncogenic NTRK fusion in a patient with soft-tissue sarcoma with response to the tropomyosin-related kinase inhibitor LOXO-101. Cancer Discov. 2015; 5:1049-57. doi: 10.1158/2159-8290.CD-15-0443
25. Morrison KB, Tognon CE, Garnett MJ, Deal C, Sorensen PH. ETV6-NTRK3 transformation requires insulin-like growth factor 1 receptor signaling and is associated with constitutive IRS-1 tyrosine phosphorylation. Oncogene. 2002; 21:5684-95. doi: 10.1038/sj.onc.1205669
26. Hong DS, DuBois SG, Kummar S, Farago AF, Albert CM, Rohrberg KS, van Tilburg CM, Nagasubramanian R, Berlin JD, Federman N, Mascarenhas L, Geoerger B, Dowlati A, Pappo AS, Bielack S, Doz F, McDermott R, Patel JD, Schilder RJ, Tahara M, Pfister SM, Witt O, Ladanyi M, Rudzinski ER, Nanda S, Childs BH, Laetsch TW, Hyman DM, Drilon A. Larotrectinib in patients with TRK fusion-positive solid tumours: a pooled analysis of three phase 1/2 clinical trials. Lancet Oncol. 2020; 21:531-40. doi: 10.1016/S1470-2045(19)30856-3

27. Heinen TE, dos Santos RP, da Rocha A, dos Santos MP, Lopez PL, Silva Filho MA, Souza BK, Rivero LF, Becker RG, Gregianin LJ, Brunetto AL, Brunetto AT, de Farias CB, Roesler R. Trk inhibition reduces cell proliferation and potentiates the effects of chemotherapeutic agents in Ewing sarcoma. Oncotarget. 2016; 7:34860-80. doi: 10.18632/oncotarget.8992
28. Chiu HT, Chen YL, Chen CY, Jin C, Lee MN, Lin YC. Molecular cloning, sequence analysis and functional characterization of the gene cluster for biosynthesis of K-252a and its analogs. Mol Biosyst. 2009; 5:1180-1191. doi: 10.1039/b905293c
29. Kase H, Iwahashi K, Matsuda Y. K-252a, a potent inhibitor of protein kinase C from microbial origin. J Antibiot (Tokyo). 1986; 39:1059-65. doi: 10.7164/antibiotics.39.1059
30. Lazarovici P, Rasouly D, Friedman L, Tabekman R, Ovadia H, Matsuda Y. K252a and staurosporine microbial alkaloid toxins as prototype of neurotropic drugs. Adv Exp Med Biol. 1996: 391:367-77. doi: 10.1007/978-1-4613-0361-9_31
31. Nakanishi S, Yamada K, Kase H, Nakamura S, Nonomura Y. K-252a, a novel microbial product, inhibits smooth muscle myosin light chain kinase. J Biol Chem. 1988; 263:6215-9
32. Gschwendt M, Leibersperger H, Marks F. Differentiative action of K252a on protein kinase C and a calcium-unresponsive, phorbol ester/phospholipid-activated protein kinase. Biochem Biophys Res Commun. 1989; 164:974-82. doi: 10.1016/0006-291x(89)91765-8
33. Hashimoto Y, Nakayama T, Teramoto T, Kato H, Watanabe T, Kinoshita M, Tsukamoto K, Tokunaga K, Kurokawa K, Nakanishi S, et al. Potent and preferential inhibition of Ca2+/calmodulin-dependent protein kinase II by K252a and its derivative, KT5926. Biochem Biophys Res Commun. 1991; 181:423-9. doi: 10.1016/s0006-291x(05)81436-6
34. Mizuno K, Saido TC, Ohno S, Tamaoki T, Suzuki K. Staurosporine-related compounds, K252a and UCN-01, inhibit both cPKC and nPKC. FEBS Lett. 1993; 330:114-6. doi: 10.1016/0014-5793(93)80254-r
35. Pan J, Wang G, Yang HQ, Hong Z, Xiao Q, Ren RJ, Zhou HY, Bai L, Chen SD. K252a prevents nigral dopaminergic cell death induced by 6-hydroxydopamine through inhibition of both mixed-lineage kinase 3/c-Jun NH2-terminal kinase 3 (JNK3) and apoptosis-inducing kinase 1/JNK3 signaling pathways. Mol Pharmacol. 2007; 72:1607-18. doi: 10.1124/mol.107.038463
36. Tapley P, Lamballe F, Barbacid M. K252a is a selective inhibitor of the tyrosine protein kinase activity of the trk family of oncogenes and neurotrophin receptors. Oncogene. 1992; 7:371-81
37. Drilon A, Nagasubramanian R, Blake JF, Ku N, Tuch BB, Ebata K, Smith S, Lauriault V, Kolakowski GR, Brandhuber BJ, Larsen PD, Bouhana KS, Winski SL, Hamor R, Wu WI, Parker A, Morales TH, Sullivan FX, DeWolf WE, Wollenberg LA, Gordon PR, Douglas-Lindsay DN, Scaltriti M, Benayed R, Raj S, Hanusch B, Schram AM, Jonsson P, Berger MF, Hechtman JF, Taylor BS, Andrews S, Rothenberg SM, Hyman DM. A next-generation TRK kinase inhibitor overcomes acquired resistance to prior TRK kinase inhibition in patients with TRK fusion-positive solid tumors. Cancer Discov. 2017; 7:963-72. doi: 10.1158/2159-8290.CD-17-0507
38. MacFarland SP, Naraparaju K, Iyer R, Guan P, Kolla V, Hu Y, Tan K, Brodeur GM. Mechanisms of entrectinib resistance in a neuroblastoma xenograft model. Mol Cancer Ther. 2020; 19:920-6. doi: 10.1158/1535-7163.MCT-18-1044

39. Chmelařová M, Dvořáková E, Špaček J, Laco J, Mžik M, Palička V. Promoter methylation of GATA4, WIF1, NTRK1 and other selected tumour suppressor genes in ovarian cancer. Folia Biol (Praha). 2013; 59:87-92
40. Dvořák O, Slavíčková M, Laco J, Štěpán M, Čermáková E, Špaček J. DNA hypermethylation of tumor suppressor genes TWIST1, GATA4, MUS81 and NTRK1 in endometrial hyperplasia. Ceska Gynekol. 2024; 89:261-8. doi: 10.48095/cccg2024261
41. Luo Y, Kaz AM, Kanngurn S, Welsch P, Morris SM, Wang J, Lutterbaugh JD, Markowitz SD, Grady WM. NTRK3 is a potential tumor suppressor gene commonly inactivated by epigenetic mechanisms in colorectal cancer. PLoS Genet. 2013;9:e1003552. doi: 10.1371/journal.pgen.1003552
42. Ji H, Li K, Jiang W, Li J, Zhang JA Zhu X. MRVI1 and NTRK3 are potential tumor suppressor genes commonly inactivated by DNA methylation in cervical cancer. Front Oncol. 2022; 11:802068. doi: 10.3389/fonc.2021.802068
43. Kim MS, Lee WS, Lee H, Jin W. TrkC, a novel prognostic marker, induces and maintains cell survival and metastatic dissemination of Ewing sarcoma by inhibiting EWSR1-FLI1 degradation. Cell Death Dis. 2022; 13:836. doi: 10.1038/s41419-022-05275-w
44. Lam SW, Briaire-de Bruijn IH, van Wezel T, Cleven AHG, Hogendoorn PCW, Cleton-Jansen AM, Bovée JVMG. NTRK fusions are extremely rare in bone tumours. Histopathology. 2021; 79:880-5. doi: 10.1111/his.14432
45. Anderson PM, Bielack SS, Gorlick RG, Skubitz K, Daw NC, Herzog CE, Monge OR, Lassaletta A, Boldrini E, Pápai Z, Rubino J, Pathiraja K, Hille DA, Ayers M, Yao SL, Nebozhyn M, Lu B, Mauro D. A phase II study of clinical activity of SCH 717454 (robatumumab) in patients with relapsed osteosarcoma and Ewing sarcoma. Pediatr Blood Cancer. 2016; 63:1761-70. doi: 10.1002/pbc.26087
46. Juergens H, Daw NC, Geoerger B, Ferrari S, Villarroel M, Aerts I, Whelan J, Dirksen U, Hixon ML, Yin D, Wang T, Green S, Paccagnella L, Gualberto A. Preliminary efficacy of the anti-insulin-like growth factor type 1 receptor antibody figitumumab in patients with refractory Ewing sarcoma. J Clin Oncol. 2011; 29:4534-40. doi: 10.1200/JCO.2010.33.0670
47. Naing A, LoRusso P, Fu S, Hong DS, Anderson P, Benjamin RS, Ludwig J, Chen HX, Doyle LA, Kurzrock R. Insulin growth factor-receptor (IGF-1R) antibody cixutumumab combined with the mTOR inhibitor temsirolimus in patients with refractory Ewing's sarcoma family tumors. Clin Cancer Res. 2012; 18:2625-31. doi: 10.1158/1078-0432.CCR-12-0061
48. Olmos D, Postel-Vinay S, Molife LR, Okuno SH, Schuetze SM, Paccagnella ML, Batzel GN, Yin D, Pritchard-Jones K, Judson I, Worden FP, Gualberto A, Scurr M, de Bono JS, Haluska P. Safety, pharmacokinetics, and preliminary activity of the anti-IGF-1R antibody figitumumab (CP-751,871) in patients with sarcoma and Ewing's sarcoma: a phase 1 expansion cohort study. Lancet Oncol. 2010; 11:129-35. doi: 10.1016/S1470-2045(09)70354-7
49. Pappo AS, Patel SR, Crowley J, Reinke DK, Kuenkele KP, Chawla SP, Toner GC, Maki RG, Meyers PA, Chugh R, Ganjoo KN, Schuetze SM, Juergens H, Leahy MG, Geoerger B, Benjamin RS, Helman LJ, Baker LH. R1507, a monoclonal antibody to the insulin-like growth factor 1 receptor, in patients with recurrent or refractory Ewing sarcoma family of tumors: results of a phase II Sarcoma Alliance for Research through Collaboration study. J Clin Oncol. 2011; 29:4541-7. doi: 10.1200/JCO.2010.34.0000

50. Tap WD, Demetri G, Barnette P, Desai J, Kavan P, Tozer R, Benedetto PW, Friberg G, Deng H, McCaffery I, Leitch I, Badola S, Chang S, Zhu M, Tolcher A. Phase II study of ganitumab, a fully human anti-type-1 insulin-like growth factor receptor antibody, in patients with metastatic Ewing family tumors or desmoplastic small round cell tumors. J Clin Oncol. 2012; 30:1849-56. doi: 10.1200/JCO.2011.37.2359
51. Li H, Zhang P, Fu G, Li J, Liu H, Li Z. Alterations in tyrosine kinase receptor (Trk) expression induced by insulin-like growth factor-1 in cultured dorsal root ganglion neurons. Brain Res Bull. 2013; 90:25-34. doi: 10.1016/j.brainresbull.2012.09.011
52. Assi A, Farhat M, Mohanna R, Hachem MCR, Zalaquett Z, Aoun M, Farraj SA, Daher M, Sebaaly A, Kourie HR. Tyrosine kinase inhibitors in Ewing's sarcoma: a systematic review. BMC Cancer. 2025; 25:735. doi: 10.1186/s12885-025-14130-y
53. Teicher BA, Bagley RG, Rouleau C, Kruger A, Ren Y, Kurtzberg L. Characteristics of human Ewing/PNET sarcoma models. Ann Saudi Med. 2011; 31:174-82. doi: 10.4103/0256-4947.78206
54. Adnani M, Hong SH, Galli S, Mahajan A, Lu C, Abualsaud N, Biermann T, Li Y, Rivera A, Sebsebie BS, Caprio L, Kuwahara L, Krawczyk E, Tilan JU, Lee Y, Rodriguez O, Wang H, Jin L, Regan M, de Assis S, Albanese C, Pack SD, Cavalli LR, Kitlinska J. Targeted CRISPR approach reveals an essential role for neuropeptide Y receptor Y5 in Ewing sarcoma extrapulmonary metastasis. Oncogene. 2025; 44:3350-63. doi: 10.1038/s41388-025-03493-y
55. Lin MY, Damron TA, Horton JA. Cell cycle arrest and apoptosis are early events in radiosensitization of EWS::FLI1+ Ewing sarcoma cells by Mithramycin A. Int J Radiat Biol. 2023; 99:1570-83. doi: 10.1080/09553002.2023.2188930
56. Dela Cruz FS, Stewart EA, Surdez D, Daley JD, Soragni A, Tomazou EM, Alvarez-Perez J, Feinberg TY, Amatruda JF, Ganapathi SS, Ohm JE, Heske CM, Cohen-Gogo S, Pesic D, Nash JO, Shlien A, Roundhill EA, Burchill SA, Crompton BD, Lawlor ER, Loeb DM, Delattre O, Mora J, Scotlandi K, Reed DR, Grohar PJ, Grünewald TGP, Kovar H, Bailey KM. Advancing preclinical biology for Ewing sarcoma: An international effort. Mol Cancer Ther. 2025; OF1-OF23. doi: 10.1158/1535-7163.MCT-25-0428
57. Zheng S, Wang W, Aldahdooh J, Malyutina A, Shadbahr T, Tanoli Z, Pessia A, Tang J. SynergyFinder Plus: Toward better interpretation and annotation of drug combination screening datasets. Genomics Proteomics Bioinformatics. 2022, 20:587-96. doi: 10.1016/j.gpb.2022.01.004
58. Volchenboum SL, Andrade J, Huang L, Barkauskas DA, Krailo M, Womer RB, Ranft A, Potratz J, Dirksen U, Triche TJ, Lawlor ER. Gene expression profiling of Ewing sarcoma tumors reveals the prognostic importance of tumor-stromal interactions: A report from the Children's Oncology Group. J Pathol Clin Res. 2015; 1:83-94. doi: 10.1002/cjp2.9

## LEGENDS FOR FIGURES

**Figure 1: Treatment with K252a delays ES tumor growth.** (**A**) Schematic of the experimental design. Human SK-ES-1 ES cells were xenografted into nude mice and the tumors were allowed to grow for 18 days. (**B**) tumor volume across experimental days. The blue line represents control mice and the pink line represents mice given K252a. The number of alive animals in each experimental day was: day 0, control, $n$ = 14; K252a, $n$ = 13; day 3, control, $n$ = 14; K252a, $n$ = 13; day 6, control, $n$ = 14; K252a, $n$ = 13; day 9, control, $n$ = 14; K252a, $n$ = 13; day 12, control, $n$ = 14; K252a, $n$ = 12; day 15, control, $n$ = 11; K252a, $n$ = 9; day 18, control, $n$ = 7; K252a, $n$ = 7; * $p < 0.05$, ** $p < 0.01$, comparisons between experimental days in each group. (**C**) Representative tumors from controls and K252-treated mice. (**D**) Body weight across experimental days; Serum levels of (**E**) AST, (**F**) ALT, (**G**) urea, and (**H**) creatinine in controls and K252a-treated mice ($n$ = 7 per group).

**Figure 2: Immunohistochemical expression of total (phosphorylated and non-phosphorylated, t) (A, E) TrkA, (B, F) TrkB, (C, G) TrkC, and (D, H) PI3K in ES tumors from controls and K252a-treated mice (n = 7 per group).** (**A-D**) Representative micrographs, X 40. (**E-H**) Protein content was quantified and shown as mean + S.E.M. optical density; $p$ values are indicated in the panels.

**Figure 3: Immunohistochemical expression of phosphorylated (p) (A, E) TrkA, (B, F) TrkB, (C, G) TrkC, and (D, H) PI3K in ES tumors from controls and K252a-treated mice (*n* = 7 per group).** (**A-D**) Representative micrographs, X 40. (**E-H**) Protein content was quantified and shown as mean + S.E.M. optical density; $p$ values are indicated in the panels.

**Figure 4: IGF1R expression and interaction with K252a in ES tumors. (A) Representative micrographs (X 40) of immunohistochemical expression for total (t-IGF1R) and phosphorylated (p-IGF1R) IGF1R in controls and K252a-treated mice (*n* = 7 per group).** (**B**) Protein content was quantified and shown as mean + S.E.M. optical density; $p$ values are indicated in the panels. (**C**) Viability of SK-ES-1 ES cells treated with K252a (10 nM), the IGF1R inhibitor NVP-ADW742 (196.6 nM), or the two inhibitors combined. Cell viability was assessed by a trypan blue cell counting assay; $n$ = 3 independent experiments, $p < 0.05$. (**D**) ZIP synergism score for the combination of K252a and NVP-ADW742.

**Figure 5: Associations between NTRK gene expression and prognosis assessed by OS in patients with ES.** Datasets GSE63155 and GSE63156, comprising expression data from 46 primary ES tumors biopsies from COG and 39 tumors from the EuroEwing collaborative group respectively [58] were used (**A**) NTRK1, COG; (**B**) NTRK1, EuroEwing, (**C**) NTRK2, COG; (**D**) NTRK2, EuroEwing, (**E**) NTRK3, COG; (**F**) NTRK3, EuroEwing; $p$ values are indicated in each panel.

**Figure 6: Schematic model highlighting selected aspects of K252a effects on ES.** Systemic administration of K252a delays the growth of human SK-ES-1 ES tumors xenografted into nude mice and the effect is associated with reduced expression and

phosphorylation of TrkA, TrkB, PI3K, and IGF1R in the tumors. Combined exposure to K252a and the IGF1R inhibitor NVP-ADW742 reduces SK-ES-1 ES cell viability more effectively than each compound alone.

**Figure 1**

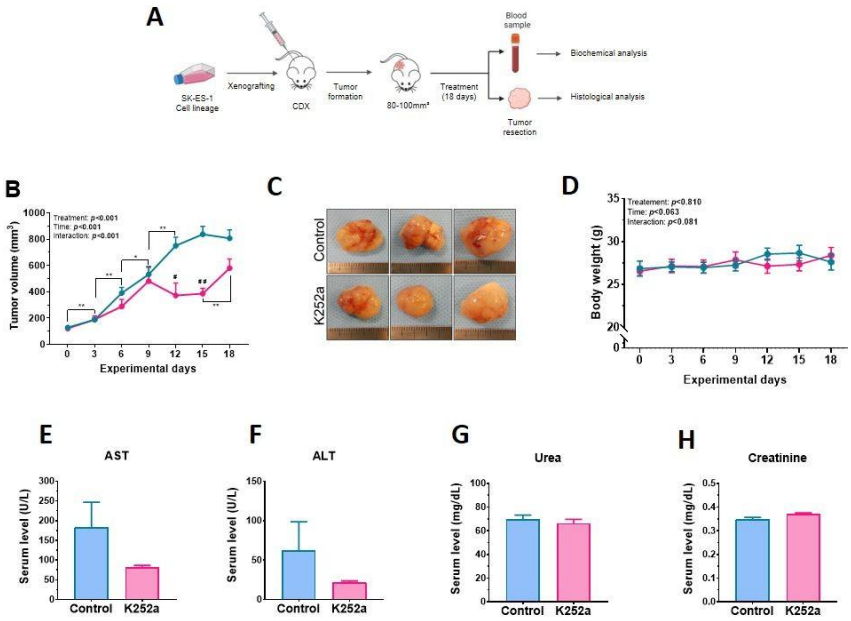
A
SK-ES-1 Cell lineage
Xenografting
CDX
Tumor formation
80-100mm³
Treatment (18 days)
Blood sample
Biochemical analysis
Tumor resection
Histological analysis
B
Treatment: p<0.001
Time: p<0.001
Interaction: p<0.001
Tumor volume (mm³)
Experimental days
C
Control
K252a
D
Treatement: p<0.810
Time: p<0.063
Interaction: p<0.081
Body weight (g)
Experimental days
E
AST
Serum level (U/L)
Control
K252a
F
ALT
Serum level (U/L)
Control
K252a
G
Urea
Serum level (mg/dL)
Control
K252a
H
Creatinine
Serum level (mg/dL)
Control
K252a

**Figure 2**

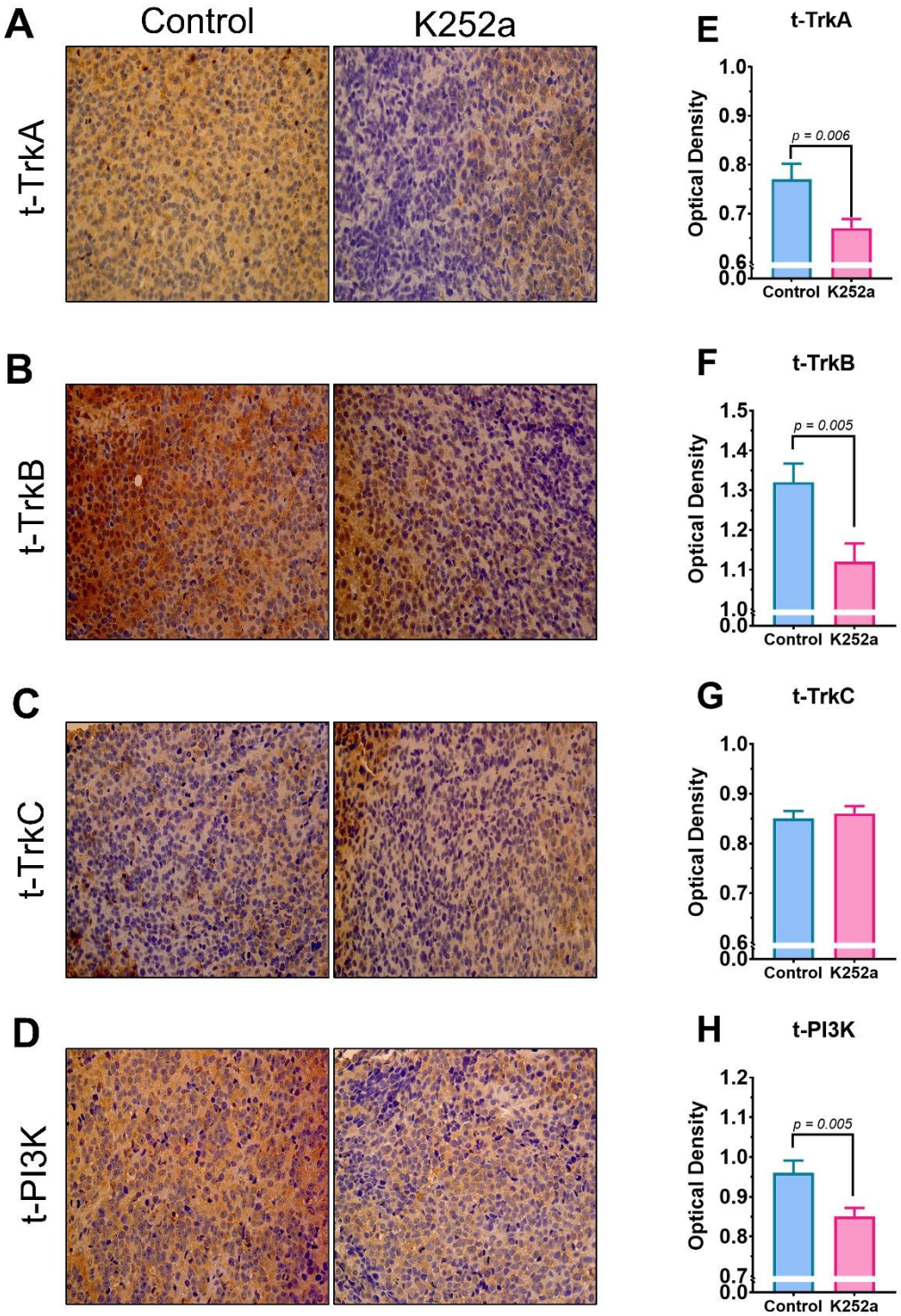
A
Control
K252a
t-TrkA
B
t-TrkB
C
t-TrkC
D
t-PI3K
E
t-TrkA
Optical Density
p = 0.006
Control
K252a
F
t-TrkB
p = 0.005
G
t-TrkC
H
t-PI3K
p = 0.005

**Figure 3**

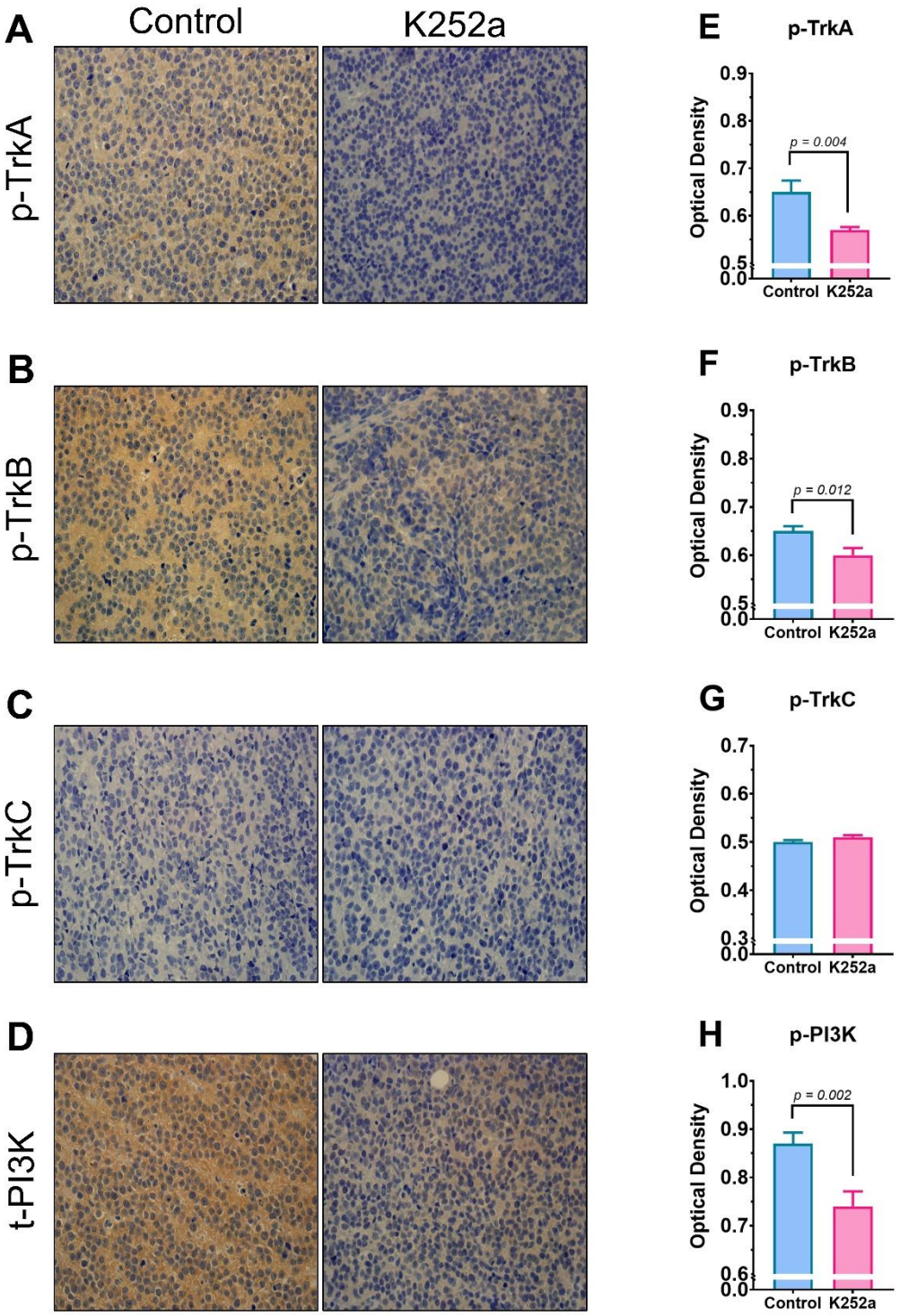
A
Control
K252a
p-TrkA
B
p-TrkB
C
p-TrkC
D
t-PI3K
E
p-TrkA
Optical Density
p = 0.004
Control
K252a
F
p-TrkB
p = 0.012
G
p-TrkC
H
p-PI3K
p = 0.002

**Figure 4**

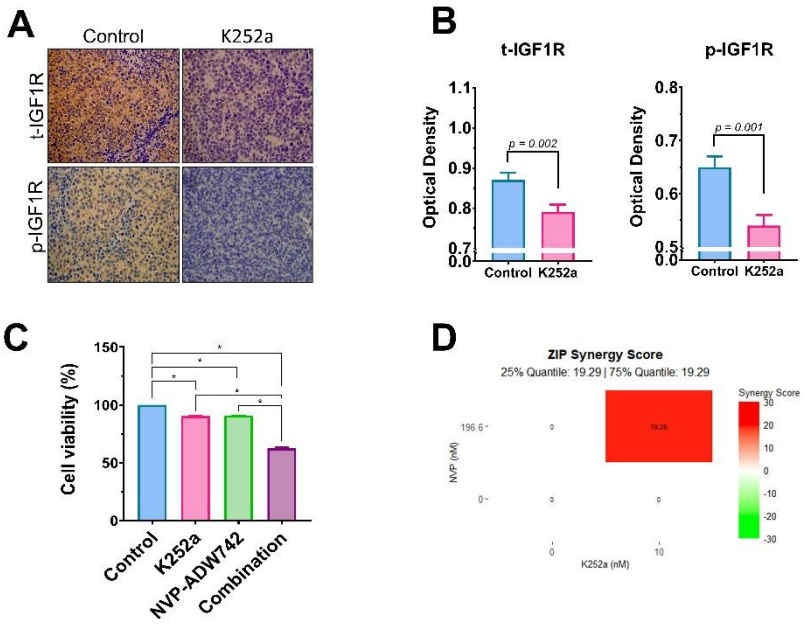
A
Control
K252a
t-IGF1R
p-IGF1R
B
t-IGF1R
p-IGF1R
Optical Density
p = 0.002
p = 0.001
Control
K252a
C
Cell viability (%)
Control
K252a
NVP-ADW742
Combination
D
ZIP Synergy Score
25% Quantile: 19.29 | 75% Quantile: 19.29
Synergy Score
NVP (nM)
K252a (nM)

**Figure 5**

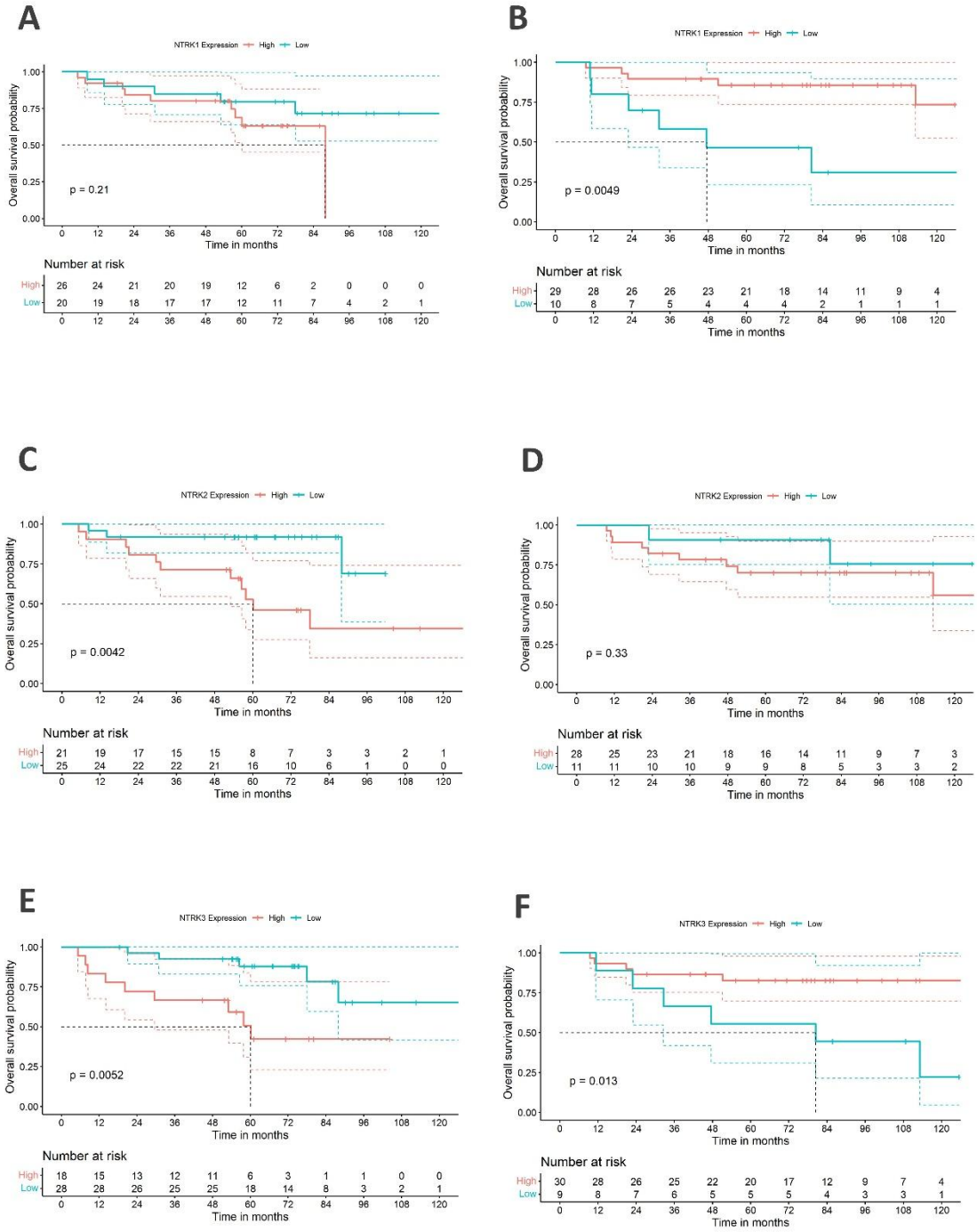
A
NTRK1 Expression High Low
Overall survival probability
p = 0.21
Time in months
Number at risk
High 26 24 21 20 19 12 6 2 0 0 0
Low 20 19 18 17 17 12 11 7 4 2 1
0 12 24 36 48 60 72 84 96 108 120
B
NTRK1 Expression High Low
Overall survival probability
p = 0.0049
Time in months
Number at risk
High 29 28 26 26 23 21 18 14 11 9 4
Low 10 8 7 5 4 4 4 2 1 1 1
0 12 24 36 48 60 72 84 96 108 120
C
NTRK2 Expression High Low
Overall survival probability
p = 0.0042
Time in months
Number at risk
High 21 19 17 15 15 8 7 3 3 2 1
Low 25 24 22 22 21 16 10 6 1 0 0
0 12 24 36 48 60 72 84 96 108 120
D
NTRK2 Expression High Low
Overall survival probability
p = 0.33
Time in months
Number at risk
High 28 25 23 21 18 16 14 11 9 7 3
Low 11 11 10 10 9 9 8 5 3 3 2
0 12 24 36 48 60 72 84 96 108 120
E
NTRK3 Expression High Low
Overall survival probability
p = 0.0052
Time in months
Number at risk
High 18 15 13 12 11 6 3 1 1 0 0
Low 28 28 26 25 25 18 14 8 3 2 1
0 12 24 36 48 60 72 84 96 108 120
F
NTRK3 Expression High Low
Overall survival probability
p = 0.013
Time in months
Number at risk
High 30 28 26 25 22 20 17 12 9 7 4
Low 9 8 7 6 5 5 5 4 3 3 1
0 12 24 36 48 60 72 84 96 108 120

**Figure 6**

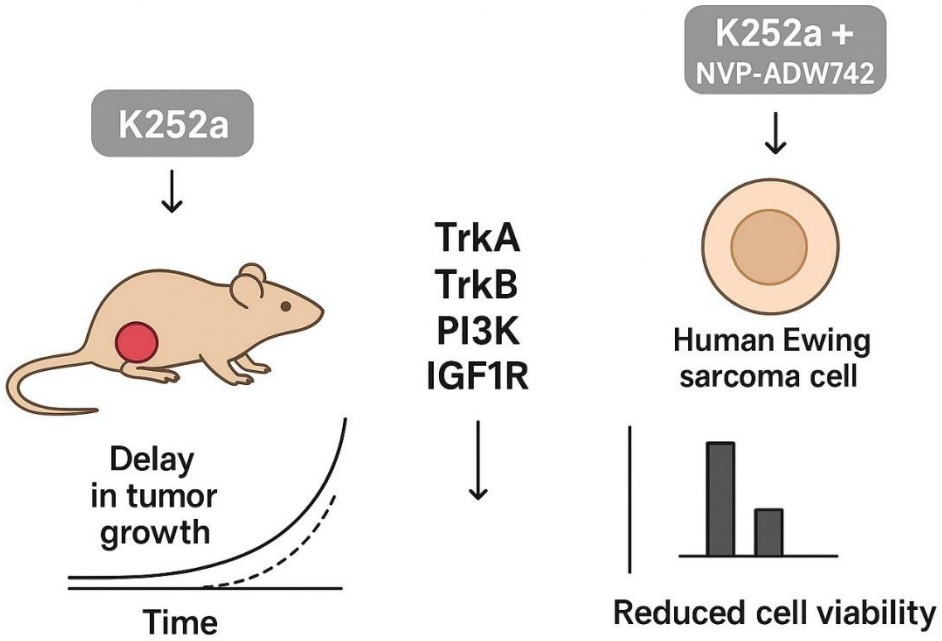
K252a
Delay
in tumor
growth
Time
TrkA
TrkB
PI3K
IGF1R
K252a +
NVP-ADW742
Human Ewing
sarcoma cell
Reduced cell viability